Polymer Bulletin (2023) 80:6197–6219
https://doi.org/10.1007/s00289-022-04308-w

ORIGINAL PAPER

# Preparation, Characterization and In vitro Biological activity of 5-Fluorouracil Loaded onto poly (D, L-lactic-co-glycolic acid) Nanoparticles

**Moshera Samy[1] · Heba M. Abdallah[1] · Hanem M. Awad[2] · Magdy M. H. Ayoub[1]**

Received: 13 February 2022 / Revised: 7 May 2022 / Accepted: 26 May 2022 /
Published online: 9 July 2022


## Abstract

Nanoscale devices offer a lot of potential in drug delivery because of their small size. The goal of this work was to increase the oral bioavailability of the anti-cancer hydrophilic drug as 5-fluorouracil (5-FU) by incorporating it into poly (D, L-lactide-co-glycolide) nanoparticles (PLGNPs) using the double emulsion process, 5-FU- PLGNPs nanoparticles were created. Various factors, such as drug, polymer, and stabilizer concentrations, were investigated for assembly in order to arrive at the most effective formulation of 5-FU-PLGNPs. PLGNPs had a drug encapsulation efficiency of 9.75 to 24.8%. The prepared nanoparticles had a spherical shape and an average size of 212.3–285 nm, as shown by TEM. The dispersion of the drug into the prepared PLGNPs was confirmed by XRPD and FTIR. The optimized nanoparticles (F225) had high encapsulation efficiency $24.8 \pm 0.21\%$, low particles size $212.3 \pm 48.2$ nm with an appropriate PDI value of 0.448, and ZP of $-48.3 \pm 2.7$ mV. The molecular dispersion of the medication within the system was validated by thermal behavior studies (DSC). In vitro drug release from the best-selected formulations revealed a sustained release of nanoparticles, with slower release reported when lower PVA concentrations were utilized. Three 5-FU-PLGNPs formulations were tested for anticancer efficacy against cell cultures of HCT-116 (human colorectal carcinoma), MCF-7 (human breast carcinoma), and HepG2 (human hepatocellular carcinoma). The created formulations were examined for in vitro cytotoxic activity, revealing that they appeared to be promising effective anticancer formulations when compared to the positive controlled (doxorubicin).

**Keywords** 5-Fluorouracil, poly (D, L-lactic-co-glycolic acid), double emulsion · HCT-116 · MCF-7 · HepG2 · Cytotoxicity

✉ Moshera Samy
moshera_samy1984@yahoo.com

[1] Polymer and Pigments Departments, National Research Centre, Dokki 12622, Giza, Egypt

[2] Tanning Materials and Leather Technology Department, Centre of Excellence, National Research Centre, Dokki 12622, Giza, Egypt

## Introduction

Cancer is the largest cause of mortality in developed countries and one of the most stimulating diseases to cure [1]. Despite the increasing number of nanoscale technologies, it has remained a global health hazard during the last decade [2]. Chemotherapy is the most common treatment for both localized and metastasized cancers. Even though the development of both diagnostic and therapeutic tools is increasing, nonselective drug distribution, increased drug toxicity, and undesirable side effects of normal tissues exacerbate the challenges of chemotherapy. To get around this, carrier-mediated drug delivery offers a variety of design options for customizing a drug's delivery for improved therapeutic impact [3]. It has been confirmed that the encapsulating of these anticancer drugs in nanometer-sized particles allows for controlled release. As a result, nanotechnology can be used to extend the life expectancy of cancer patients in the field of chemotherapy. 5-FU is one of a broad-spectrum anticancer drugs [4–6] that is used to treat a variety of solid tumors including those of the breast, pancreas, colorectal ovary, head, liver, kidney, stomach, neck, and glioblastoma [7–9]. Because 5-FU inhibits with DNA synthesis, it is generally used as a thymidylate synthase inhibitor [10, 11]. on the other hand, 5-FU, has a low bioavailability, lacks specificity, and has a short plasma half-life. As a result, excessive doses are used, resulting in side effects and so many undesirable effects such as severe anemia, diarrhea and vomiting [12–14]. The clinical use of 5-FU has been severely limited due to improved cancer cell resistance [15, 16].

The incorporation of 5-FU into polymeric nanoparticles is one way to solve this problem. These drug delivery carriers have special characteristics, such as the potential to adjust their surface properties, improve drug stability, and preserve the entrapped drug [17]. Additionally, biodegradable polymeric nanoparticles can improve drug bioavailability, drug release control, and cell and tissue selectivity [18]. There has been a rise in interest in drug delivery research in recent years. Several research employing biodegradable polymers like poly (D, L-lactic-co-glycolic acid) (PLGA), which are very useful due to their biodegradability and biocompatibility, have been conducted on sustained drug delivery systems for 5-FU [19]. Because of FDA permission, it is commonly used in human research (Food and Drug Administration, USA). For more than a decade, it has been successfully utilized as a drug carrier for a variety of drugs, including 5-FU [20].

PLGA nanoparticles (PLGNPs) are colloidal polymeric drug carriers that show promise for oral drug delivery, which is by far the most common and convenient route of administration. PLGNPs have various advantages over traditional oral dosage forms, including improving the oral bioavailability of poorly absorbed medicines and preserving the encapsulated drugs in the polymer network. PLGNPs were made utilizing the double emulsion approach to overcome the problems described above [21]. 5-FU-PLGNPs have the ability to penetrate into connective tissues and internalize cells without blocking capillaries. Furthermore, these nanoparticles can pass through the vasculature and accumulate in solid tumors due to leaky endothelial tissues surrounding the tumor. According to studies, nanoparticles containing anticancer drugs have a longer drug retention time in tumors, which slows

tumor growth and so extends the life of tumor-bearing animals [22–24]. Although research's are underway to improve 5-FU bioavailability using nanoparticle carrier systems, no data on the biological efficacy of PLGA nanoparticles as a 5-FU carrier has been published [25, 26].

The major goal of this research was to create a PLGA-based nanoparticle delivery system to account for numerous parameters that influence the formation of 5-FU-loaded PLGNPs as well as their efficiency as 5-FU carriers. The effect of parameters such as drug, polymer, and stabilizer concentrations for 1st emulsion and 2nd emulsion of the emulsification process on nanoparticles suspension properties. A particle size analyzer and a transmission electron microscope (TEM) were used to determine the size, shape, and charge of these nanoparticles. Differential scanning calorimetry (DSC) and X-ray diffraction (XRD) were used to investigate the thermal behavior and crystallinity, respectively. To compare the rate of 5-FU release from PLGNPs, in vitro drug release tests were carried out. MTT (3-[4, 5-dimethylthiazol-2-yl]-2, 5-diphenyltetrazolium bromide) assay followed by acridine orange/ethidium bromide (AO/EB) staining in both cell lines were used to assess the antitumor activity when compared to doxorubicin. Three 5-FU-PLGNPs formulations have been tested on HCT-116 (human colorectal carcinoma), MCF-7 (human breast adenocarcinoma), and HepG2 (human hepatocellular carcinoma).

## Materials and methods

### Materials

poly (D, L-lactic-co-glycolic acid) (PLGA; with co-polymerization ratios 50–50 (lactic/glycolic); $(C_3H_4O_2)_x(C_2H_2O_2)_y$; acid and hydroxy terminated, Mn 25,000; product number 808482), polyvinyl alcohol (PVA; $[–CH_2CHOH]n$; Mw = 30,000 g/mol; 87–89% hydrolyzed; m.p.200 °C; CAS: 9002-89-5), dichloromethane (DCM; $CH_2Cl_2$; Mw = 84.93 g/mol; CAS: 75-09-2), were delivered from Sigma–Aldrich, Germany and 5-Fluorouracil (5- FU; $C_4H_3FN_2O_2$; 5- Fluoropyrimidine-2,4-dione, ≥ 99%; CAS: 51-21-8) were delivered from Alfa Aesar, Germany. Potassium hydrogen phosphate ($KH_2PO_4$; CAS: 7778-77-0) was purchased from ALPHA CHEMIKA, India. Disodium hydrogen orthophosphate ($Na_2HPO_4$; CAS: 7558-79-4) was delivered from Sigma–Aldrich, Germany. Acetic acid ($CH_3COOH$; Mw = 60.05 g/mol; CAS: 64-19-7) was obtained from SHAM laboratory chemical, Syria; acetic acid is of pure grades. All other chemicals –otherwise mentioned were provided from Sigma–Aldrich, Germany and were used as received. 3-[4,5-dimethyl-2-thiazolyl)-2,5-diphenyl-2H-tetrazolium bromide (MTT). HCT-116 (human colorectal carcinoma), human liver carcinoma (HepG-2), MCF-7 (human breast adenocarcinoma) cell lines were purchased from the American Type Culture Collection (Rockville, MD, USA) and maintained in Dulbecco's Modified Eagle's Medium (DMEM) supplemented with 10% heat-inactivated fetal bovine serum (FBS), 100 U $mL^{-1}$ penicillin, and 100 U $mL^{-1}$ streptomycin. The cells were grown at 37 °C in a humidified atmosphere of 5% $CO_2$.

## Methods

### Preparation of 5-FU-PLGNPs

A double emulsion technique is commonly used to prepare the biodegradable nanoparticulate systems 5-FU-PLGNPs were attained by loading a hydrophilic anticancer drug (5-FU) into PLGA (oil phase), which was encapsulated by PVA (water phase, W1) acting as the polymer emulsifier (stabilizer) [27].

**Preparation of PVA solution** To be used as emulsion stabilizer in outer aqueous phase where PVA is the most widely used stabilizer due to its low toxicity, good water solubility, and availability in a wide range of molecular weights [28, 29]. Three different concentration PVA stock solutions (0.5, 1 and 2 wt. % stocks A, B and C) were prepared by slowly adding 2.5, 5 and 7.5 mg PVA, respectively, into 500 mL distilled water with stirring and heating at 60 °C for 40 min to obtain a clear 0.5, 1 and 2% PVA solution, respectively [29].

**Preparation of primary emulsion (Ist step)** In the first step, in order to make the primary emulsion (W1/O); Stock solutions of PLGA were prepared by slowly adding of 1.05, 1.57, 2.10 and 3.15 g PLGA, respectively, into 100 mL DCM until fully dissolved with stirring till forming a clear solution. Different conc. of 5-FU as 10, 15, 20 and 25 mg of 5-FU was dissolved in 1 ml of 0.5% Acetic acid in order to aid the dissolution of 5-FU and then 5 ml PLGA solution was added at constant (drug: polymer; 1:10). This mixture was properly homogenized using digital high speed homogenizer (T-10; model) at 20,000 rpm for 5 min using to have the first emulsion (W1/O) [29].

**Preparation of Double emulsion (2nd step)** In the second step, the primary emulsion (W1/O) was added in the outer aqueous phase (W2) containing stocks (A, B and C) PVA solutions as stabilizer with homogenization to achieve the double emulsion (W1/O/W2) [30, 31]. Also, a stable double emulsion was obtained using homogenization speeds of 20,000 rpm at 5 min for the first emulsion and 21,000 rpm at 15 min for the second emulsion determined to prepare PNs providing the lowest particle size [32]. This mixture was properly homogenized at 21,000 rpm for 15 min by using digital high speed homogenizer (T-10; model). In 2nd step, we used excess of outer aqueous phase (W2) in order to facilitate the diffusion of organic solvent from PLGA particle to outer aqueous phase. The obtained double emulsion ($W_1$/O/$W_2$) was subjected to evaporation under vacuum using rotary evaporator (Heidolph type VV2000, type WB2000, Germany) until the whole organic solvent (DCM) was removed [33]. The nanoparticles were collected and separated from the free drug in the nanoparticulates' suspension by centrifuge (Ambient centrifuge centurion scientific model: K2015, UK) at 6000 rpm for 45 min. Then, the produced nanoparticles' pellets were washed three times with ultra-pure water. The supernatant solution was used for determination of the drug encapsulation efficiency. The supernatant was kept for drug assay as described later and the [34] was lyophilised using freeze-dried and the powder was used for further analyses.

### Determination of Maximum wave length ($\lambda_{max}$) of 5-FU

The spectrophotometric assay adopted for 5-FU analysis by screening of 5-FU in the investigated solvent such as 0.5% acetic acid and phosphate buffer solution (PBS) using (Shimadzu UV spectrophotometer, 2401/PC, Japan) through a scan range of 200–400 nm. The 5-FU dissolved in investigate solvent at 10 µg/ml was screened in order to determine the $\lambda_{max}$ of 5-Fluorouracil from UV spectrum, using investigated solvent as a blank. This concentration was prepared by dilution from diluted a stock solution of (10 µg/ml) which was prepared by dissolving 10 mg of 5-FU, accurately weighed, in 10 ml investigate solvent analyzed for 5-FU content spectrophotometrically at 265 nm [34].

### MTT antiproliferative assay

The antiproliferative activities on the HepG-2, HCT-116, MCF-7 and BJ-1 were estimated by the 3-[4,5-dimethyl-2-thiazolyl)-2,5-diphenyl-2H-tetrazolium bromide (MTT) assay. This test is based on MTT cleavage by mitochondrial dehydrogenases form viable cells [35–37]. Cells were placed in a 96 well sterile microplate ($5 \times 10^4$ cells well$^{-1}$) and incubated at 37 °C in serum-free media containing dimethyl sulfoxide (DMSO) and either a series of various concentrations of each compound or doxorubicin (positive control) for 48 h before the MTT assay. After incubation, the media were removed and 40 µL MTT (2.5 mg mL$^{-1}$) was added to each well. Incubation was resumed for an additional 4 h. The purple formazan dye crystals were solubilized with 200 µL DMSO. Absorbance was measured at 590 nm in a Spectra Max Paradigm Multi-Mode microplate reader (Molecular Devices, LLC, San Jose, CA, USA). Relative cell viability was expressed as the mean percentage of viable cells compared to the untreated control cells. All experiments were conducted in technical triplicate and three biological replicates. All values were reported as mean ± SD. $IC_{50}$ were determined by SPSS Inc probit analysis (IBM Corp., Armonk, NY, USA).

## Characterization of 5-FU-loaded PLGNPs

### Determination of drug encapsulation efficiency (EE%)

In order to determine the EE% of 5-FU in the prepared nanoparticles, the combined washings after centrifugation were appropriately diluted using 0.5% acetic acid. The amount of free, unencapsulated 5-FU was measured spectrophotometrically at 265.2 nm using the regression equation of the standard calibration curve plotted employing suitable concentrations of 5-FU [32]. The amount of 5-FU encapsulated in PLGNPs w was calculated by subtracting the total drug added during the preparation of the PLGNPs from the free drug present in the supernatant from using the following formula [34, 38]

$$EE\% = \frac{\text{Free drug} - \text{Total amount of drug}}{\text{Total drug}} \times 100 \quad (1)$$

### Determination of particle size (PS) and polydispersity index (PDI)

The PS for the prepared nanoparticles was measured by means of photon correlation spectroscopy (PCS) using a Zeta-sizer (Nano ZS, Malvern Instruments Ltd., Malvern, the UK). Samples were suitably diluted with distilled water and measured at ambient temperature using quartz cuvettes. PDI were measured for each preparation (in triplicate) and the standard deviations were calculated.

### Fourier transform infrared spectroscopy

FTIR spectroscopy was used to study the chemical composition of PLGA, 5-FU, PVA as well as the selected 5-FU-loaded PLGNPs. The spectra were recorded using FTIR spectrometer (Jasco, FT/IR 6100, Japan). The KBr pellet method was employed where the powdered samples were ground and mixed with KBr then compressed into disks. To collect the data for each spectrum, 32 scans were performed in the mid-infrared range 4000–400 $cm^{-1}$.

### X-ray powder diffraction (XRPD)

The physical state of PLGA, 5-FU, PVA and selected 5-FU-loaded PLGNPs formulations was evaluated using XRPD. Measurements were acquired with X-ray diffractometer (Bruker AXS, D8 Advance, Germany) which was operated at 40 kV and 40 mA using CuKα as a radiation source where $\lambda = 1.54$ A°. The diffractograms were recorded in the diffraction angle (2θ) range between 4 and 50°, and the process parameters were set at scan step size of 0.020° and scan step time of 0.4 s.

### Thermal analysis (TA)

TA is useful for evaluating thermal properties and drug–polymer interactions to assess the influence of recipients and nano-encapsulation process on the physicochemical characteristics of the pharmaceutical materials. Differential scanning calorimetry (DSC) and thermal gravimetric analysis (TGA) are the most frequently used thermo-analytical techniques.

**Differential scanning calorimetry (DSC)** Thermal stability of freeze-dried 5-FU–PLGNPs was investigated through DSC using thermal analyzer DSC–SDT (Simultaneous DSC-TGA) Q600 V20.9 Build 20, the USA, in the range from room temperature to 500 °C at a heating rate of 10 °C/min under inert nitrogen atmosphere $N_2$ using reference alumina. The samples weight was between 2.5 and 12 mg.

**Thermal gravimetric analysis (TGA)** Thermal behavior for freeze-dried 5-FU–PLGNPs formulations was recorded using thermal analyzer TGA–SDT Q600 V20.9

Build 20, (USA) in the range from room temperature to 700 °C at a heating rate of 10 °C/min under inert nitrogen atmosphere (N*2*) using reference alumina.

### Transmission electron microscopy

The morphology of a selected 5-FU-loaded PLGNPs formulation and their dimensions in nanometer range was confirmed by transmission electron microscopy. The TEM (JEOL Co., JEM-2100, Japan) was adjusted at a high tension electricity of 200 kV. One drop of the appropriately diluted sample was placed onto a carbon-coated copper grid, negatively stained with 1% phosphotungstic acid and left to dry at ambient temperature before being examined at suitable magnifications.

### Scanning electron microscopy (SEM)

The morphology of the prepared freeze-dried nanoparticles was investigated by scanning electron microscopy (SEM) using Quanta FEG 250 (FEI Company, Holland) device. Freeze-dried nanoparticles were deposited on a flat aluminum holder and were dried at room temperature. The concerned sample in each case was finally coated under vacuum by cathodes puttering with gold for 3 min.

### In vitro drug release study

The in vitro release of 5-FU, from best prepared PLGNPs, was evaluated employing the dialysis bag technique [34] employing a dialysis tubing cellulose membrane (Visking R, SERVA Electrophoresis GmbH, Germany; Molecular weight cutoff 12.000–14.000). An amount equivalent to 2 mg of 5-FU was instilled in the dialysis bag, sealed at both ends to prevent leakage and placed in screw capped glass containers filled with 100 ml phosphate buffer solution (pH 7.4). The entire system was kept at 37 ± 0.5 °C at 100 rpm using a shaking water bath. At predetermined time intervals (1, 2, 3, 4, 6, 8, 24 and 48 h), 5 ml of the release medium was withdrawn and replaced with 5 ml of fresh buffer solution. The samples were adequately diluted and analyzed for 5-FU content spectrophotometrically at 266.4 nm [32, 34]. The cumulative percentage of drug released was determined as the ratio of the amount of released 5-FU to the amount of 5-FU initially inserted into the dialysis bag. All measurements were performed in triplicates.

### Statistical analysis

Results are presented as mean ± SD. Statistical analysis was performed by means of one-way analysis of variance (ANOVA). All experiments were repeated at least three times. All data were expressed as means ± standard deviations of sample means. The statistical significance of the differences was evaluated by one-way

analysis of variance and $P < 0.05$ was considered to indicate a statistically significant difference.

## Results and discussion

PLGNPs-based medication delivery systems are now a useful tool for controlling various acute infection phases and preventing complications and relapse. As a result, long-term treatments are useful in overcoming reasonable deficiencies [39]. Drugs given by nanospheres that specifically target infected cells should also lessen the cytotoxicity associated with unwanted drug biodistribution. Due to their size and improved antigen presentation, drug delivery systems based on PLGNPs can work better than nanoparticle-based delivery systems depending on the mode of action [40, 41]. Figure 1 shows how 5-FU-PLGNPs were successfully synthesized in the nanoscale range using a double emulsion (W1/O/W2) technique. Table 1 shows the intended formulation of PLGA nanoparticles loaded with 5-FU.

### Drug encapsulation efficiency (EE %)

In general, the EE % was calculated using the amount of encapsulated drug within the polymer matrix. The amount of active substance in a known mass of nanoparticles (NPs) is referred to as efficiency. The average values were used to calculate the results, which were based on triplicates. The EE % of six produced 5-FU loaded PLGNPs is shown in Table 1. The EE % is a measurement that indicates the percentage of drug that has been successfully entrapped. The EE percent of 5-FU in PLGNPs (F510–F225) was measured in the range of 9.75–24.8%, according to the findings.

It is clear that an increase EE% values with the increase of 5-FU concentration the first emulsion (5–25 mg/ml),with a constant concentration of stabilizer (PVA, 0.5%) and with keeping the other parameters constant for the first and second emulsion (F510, F515, F520 and F525). Also, an increase EE% values with the increase of PVA concentration the first emulsion (0.5–2%), with a constant 5-FU concentration (5-FU, 25 mg/ml) with maintaining the other parameters constant for first and second emulsion (F525, F125and F225). Also, an increase in PLGA concentration leads to an increase in 5-FU entrapment in PLGNPs; this is likely owing to an

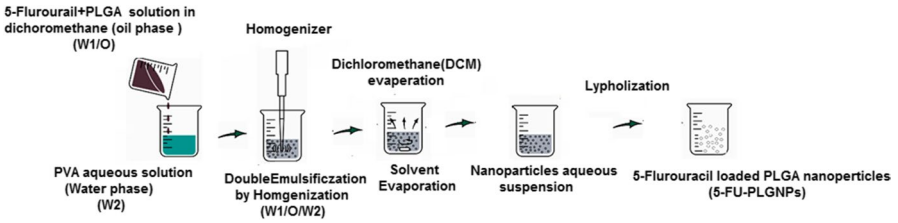


**Fig. 1** Preparation of 5-FU- PLGNPs by double emulsion technique

**Table 1** EE %, PS, PDI and ZP values of the prepared 5-FU-PLGNPs formulations

| Formulations * | 1st emulsion's factors | | 2nd emulsion's Factors | Polymer: drug ratio | EE% (±Mean SD)**** | Mean PS (nm) | PDI | ZP (mV) |
|---|---|---|---|---|---|---|---|---|
| | 5-FU conc (mg/ml)** | PLGA (gm) | PVA (%)*** | | | | | |
| F510 | 10 | 1.05 | 0.5 | 1:10 | 9.75 ± 0.14 | 239 ± 65.5 | 0.363 | − 26.3 ± 1.8 |
| F515 | 15 | 1.57 | 0.5 | 1:10 | 13.38 ± 0.43 | 240.7 ± 54.3 | 0.396 | − 30.7 ± 1.2 |
| F520 | 20 | 2.10 | 0.5 | 1:10 | 19.64 ± 0.68 | 242.9 ± 28.1 | 0.186 | − 35.9 ± 1.7 |
| F525 | 25 | 3.15 g | 0.5 | 1:10 | 23.13 ± 0.17 | 285 ± 43.1 | 0.426 | − 43.4 ± 2.1 |
| F125 | | | 1 | 1:10 | 23.56 ± 0.19 | 278.4 ± 57.3 | 0.444 | − 45.6 ± 2.6 |
| F225 | | | 2 | 1:10 | 24.8 ± 0.21 | 212.3 ± 48.2 | 0.448 | − 48.3 + 2.7 |

*All samples were prepared at homogenization speed 20,000 rpm under 5 min for 1st emulsion and15 min for 2nd emulsion at 21,000 rpm respectively

***Formulations with the initial numbers 0.5–2 represent a PVA content of 0.5, 1 or 2% emulsion, accordingly

** Formulations with the second numbers 10–25 represent a 5-FU concentration of 10, 15, 20, or 25 mg/ml in the emulsion, accordingly

****Mean SD is Mean standard deviation for each result refer to mean of three experiments

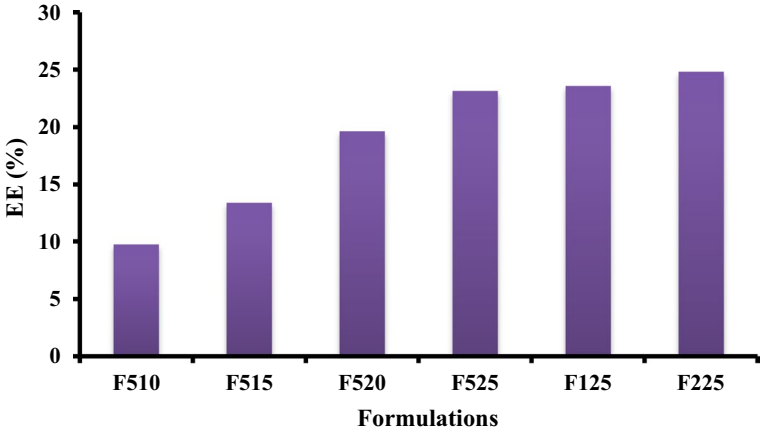


**Fig. 2** Encapsulation efficiency of 5-FU–PLGNPs formulations. The error bars are due to the triple formulation's standard deviations

increase in the viscosity of the PLGA solution, which prevents the 5-FU from diffusing into an aqueous phase. Figure 2 illustrates the EE %.

### Determination of PS, PDI, and ZP

PS, in general, has a significant impact on the carrier's biopharmaceutical properties. As a result, the PS is calculated as a function of the formulation factors. After hydration with distilled water, the particle size of the produced 5-FU-PLGNPs formulations was assessed in each case. The effect of different 5-FU concentrations (10, 15, 20, and 25 mg/ml) on the size of the NPs produced was investigated. At fixed PVA concentration, the particle size increased as the 5-FU concentration in the NPs increased. At different drug to concentrations, such as 10, 15, 20, and 25 mg/ml, respectively the sizes of NPs were $239 \pm 65.5$, $240.7 \pm 54.3$, $242.9 \pm 28.1$, $285 \pm 43.1$ nm, respectively. Particle sizes were shown to be depending on the initial concentration of 5-FU employed during the preparation procedure, according to the particle size analysis report. Previously, similar outcomes have been reported [33]. As shown in Table 1, various concentrations of PVA (0.5, 1, and 2%) were used as stabilizer. The PS of PLGNPs (F510–F225) were measured in the range of 212.3–278.4 nm. The results showed that decreasing the particle size with increasing PVA concentrations of the second emulsion from 0.5 to 2% while maintaining the 5-FU concentration of the first emulsion constant at 25 mg/ml as in case of F525, where the particle size was recorded at $285 \pm 43.1$ nm at PVA concentration 0.5%, whereas in case of F125 at PVA concentration (1%), the particle size was reduced to $278.4 \pm 57.3$ nm as shown in Table 1. Because stabilizer concentrations are a governing factor in determining the particle size created using the double emulsification technique, the reported results were in agreement with the literature [42]. (Dubey et al. 2016) Dubey's research proved that increasing the stabilizer concentration used in the production of NPs reduced particle size. The PDI is a metric

for measuring the distribution of NPs, and it ranges from 0.000 to 0.500. The PDI values for all PLGNPs ranged from 0.186 to 0.448. (Table 1). The PDI (< 0.5) of all formulations was satisfactory, indicating a restricted size distribution [42]. The ZP of the PLGNPs (F510–F525) was significantly different; the highest ZP is related to the maximum concentration of PLGA polymers used in the formulation. The ZP values were measured as − 26.3, − 30.7, − 35.9 and − 43.3 mV for F510, F515, F520 and F525, respectively (Table 1). The negative values of ZP of 5-FU-loaded PLGNPS could be attributed to ionic adsorption, modification of functional group on the particle surface or ionized reactive carboxylic functional group of the PLGA polymer. According to DLVO electrostatic theory, nanoparticles can be stable due to Brownian motion and repulsive force. At the same time, the higher ZP of either the (−) anions or (+) the cations on the NPs causes them repel each other and stabilizes the system. The pure PLGA has a ZP of about ~ ± 50 mV, however the 5-FU-loaded PLGNPs (F225) have a ZP of about − 48.3 mV, indicating a decrease in particle potential; this negative could be related to the surface adsorption of NPs with PVA.

## FTIR

FT-IR spectroscopy was used to analyze the chemical composition of PLGA 50:50 and 5-FU. The typical peaks of 5-FU, PLGA 50:50, and 5-FU-PLGNPs (F525, F125 and F225, respectively) were seen in the FT-IR spectra shown in Fig. 3. The distinctive peaks for several PLGA polymer groups were detected. The peak 1745.2 3 $cm^{-1}$ due to the C=O stretching vibration and the bands at the range of 1027.8–1186.01 $cm^{-1}$ due to the C–O stretching vibration corresponding of ester group that is present in both monomers (lactide and glycolide), were assigned to symmetric and asymmetric C–C–(=O)–O stretches, accordingly. the band at 691.3 $cm^{-1}$ due to –CH stretching vibrations, the band at 1511.9 $cm^{-1}$ due to –CH3 stretching vibrations and, the band at the range of 2931.2–2850.1 $cm^{-1}$ C–H stretching vibrations [43–45]. The broad absorption band between 3200 and 3600 $cm^{-1}$ due to O–H of hydroxyl group [46, 47]. The distinctive peaks for several 5-FU are band at around 1348 $cm^{-1}$due to pyrimidine compound vibrations whereas bands at 1179.26 and 1245.79 $cm^{-1}$ due to the C–O and C–N vibrations, respectively. Other absorption peaks were found at 3133.76 $cm^{-1}$ due to –NH Stretch. The bands at 1725.01 and 1655.59 $cm^{-1}$ due to –C=O stretching vibration, bands at 1245.79 and 809.95 $cm^{-1}$ due to CH in Plane deformation, CH out of plane deformation, respectively [45, 48]. When compared to the 5-FU peak at the same wave number, the drug's distinctive peaks in the PLGNPs (F525, F125, and F225) were reduced or shifted, confirming that 5-FU interacts with PLGA and that 5-FU is present in the PLGNPs.

## X-ray powder diffraction (XRPD)

The crystalline or amorphous nature of the 5-FU encapsulated in the PLGA nanoparticles was investigated using XRPD. To investigate the crystallinity of 5-FU

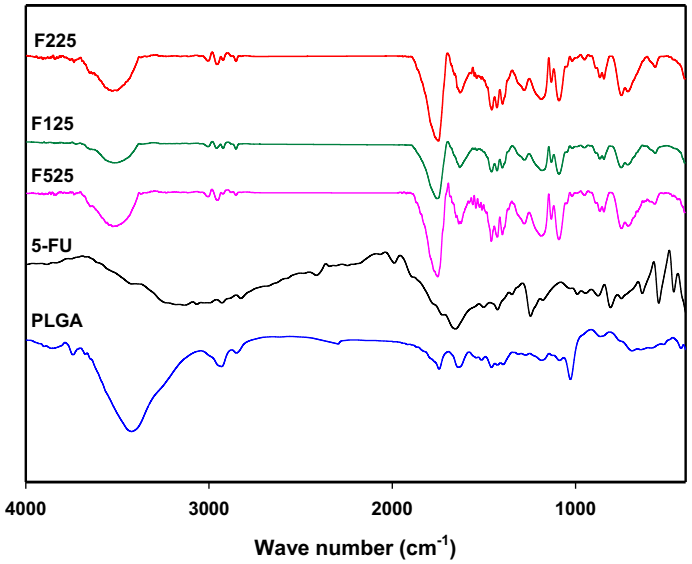


**Fig. 3** FTIR spectra of 5-FU, pure PLGA, and 5-FU–PLGNPs prepared by double emulsion technique for F525, F125 and F225, respectively

contained in the PLGA matrix, an XRPD analysis is required. PVA, 5-FU, PLGA, and 5-FU- PLGNPs (F525, F125, and F225) XRPD patterns were obtained and compared. PVA displayed several sharp signals, demonstrating its amorphous nature, as shown in Fig. 4. The diffraction plot of 5-FU revealed an intense multiple peak at 2θ values16.1, 19.8, 21.6, 22.1, 28.4, 32.7, 36.7, 36.9, and 46.5°, due to its crystalline form, whereas the diffraction plot of PLGA revealed no sharp peaks, indicating its amorphous nature. The drug's distinguishable peaks vanished in the diffraction pattern of 5-FU-PLGNPs (F525, F125, and F225), indicating that the 5-FU were encapsulated.

## Thermal analyses

The physical and chemical characteristics of 5-FU in PLGNPs are normally quantified and qualitatively assessed using TGA and DSC techniques.

### DSC

DSC is primarily used to evaluate changes in enthalpy as a function of temperature in a substance's physical and chemical properties. Figure 5 shows the enthalpy changes and final melting temperatures obtained from DSC thermograms. The glass transition temperature (Tg) of pure PLGA was 74.34 °C [43], while the $T_m$ of PVA was 290.52 °C. The melting of 5-FU was represented by the DSC curve of 5-FU, which showed a similar peak at endothermic peak

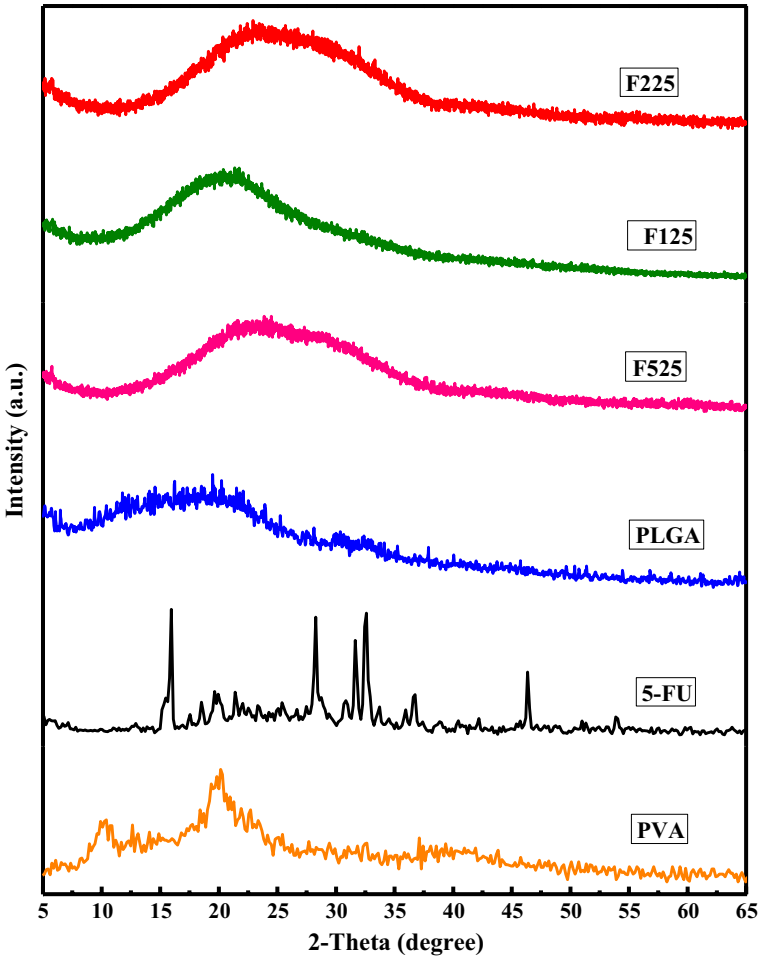


**Fig. 4** XRPD patterns of (**a**): PVA, 5-FU, pure PLGA, and (**b**): 5-FU–PLGNPs prepared by double emulsion technique for F525, F125 and F225

temperature of 282.80 °C [49, 50]. DSC thermograms for various formulations of 5-FU–PLGNPs, as shown in Table 1, Fig. 5, demonstrated disappearance of the distinguished band for 5-FU at $T_m$ of 282.80 °C, supporting XRPD results of 5-FU in molecular dispersion inside the PLGA matrix as previously reported in the literature [51].

## TGA

TGA offers information on mass loss as a function of temperature in most cases. The TGA thermograms for PLGA, PVA, and 5-FU are displayed in Fig. 6. The decomposition of 5-FU took place in two stages. The decomposition process was

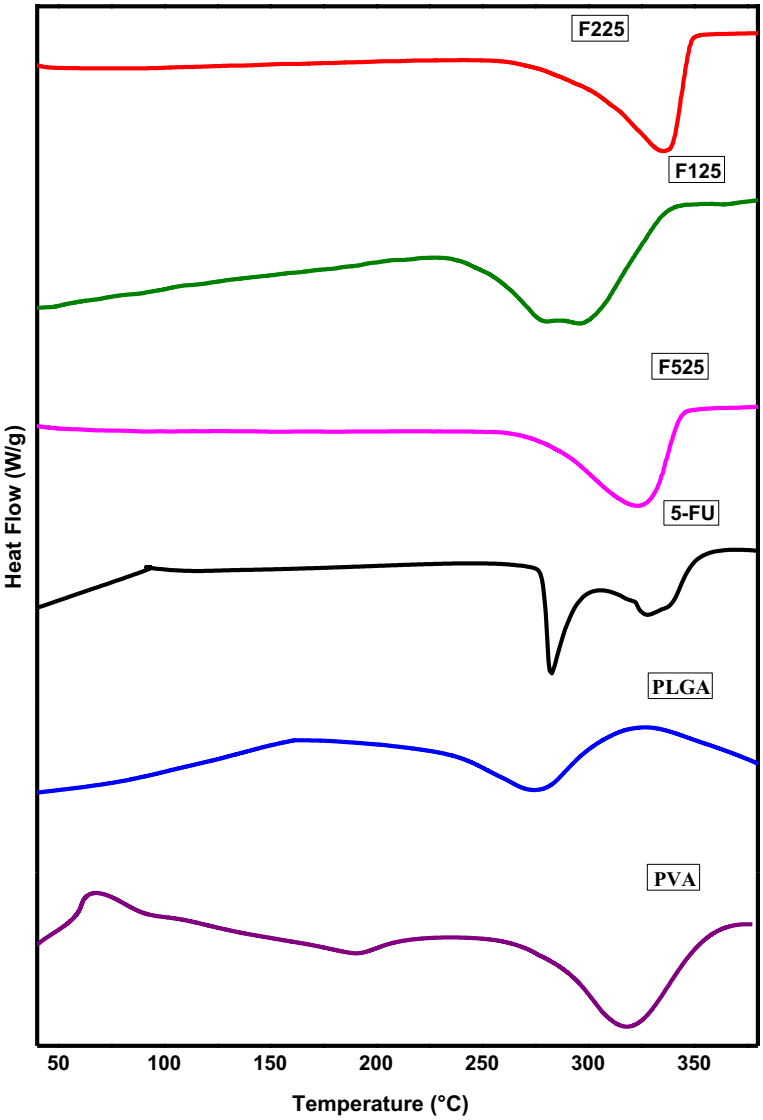


**Fig. 5** DSC thermograms of (**a**): PVA, pure PLGA and 5-FU, and (**b**): 5-FU- PLGNPs (F525, F125 and F225) at a heating rate of 10 °C/ min

performed at temperatures of 46–225 and 225–500 °C, respectively, with weight losses of 0.6 and 85.77% due to water loss. PLGA was thermal stable until 200 °C with a weight loss of 3.88%, after which it decomposed in one step from 200 to 380 °C with a weight loss of 3.03%. The degradation products of PLGA are similar to those of poly(lactide) and poly(glycolide) polymers in their pure state [52]. Fig. 6 depicts a modest decrease in thermal stability of 5-FU-PLGNPs when compared to pure PLGA. Because 5-FU ions take up a lot of space between polymeric chains,

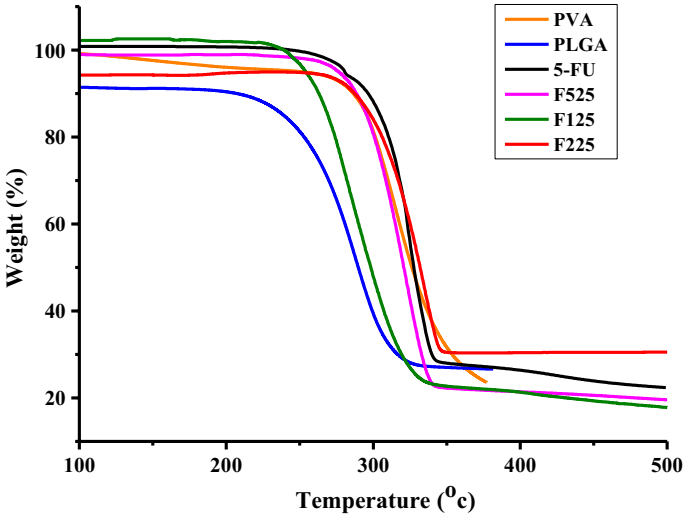


**Fig. 6** TGA thermograms of PVA, PLGA, pure 5-FU, and 5-FU–PLGNPs at a heating rate of 10 °C/min

they may inhibit interactions between them. It is clear from this observation that the adsorbent was thermally stable, and that the addition of 5-fluorouracil had no effect on the biopolymer's thermal stability.

### Transmission electron microscopy (TEM)

Figure 7 shows TEM micrographs was used to examine the shape of formulations of 5-FU-PLGNPs as F525, F125, and F225 at different PVA concentration (0.5, 1 and 2% respectively). The nanoparticles were spherical, with a narrow size distribution as shown in the micrographs.

### Scanning electron microscopic (SEM)

SEM was used to study the morphology of samples of 5-FU-PLGNPs as F525, F125, and F225 at different stabilizer PVA concentrations (0.5, 1 and 2%, respectively) as shown in Fig. 8. All nanoparticles had a round and spherical shape, a smooth surface, and a unimodel size distribution, according to SEM pictures. In the case of the second emulsion, SEM revealed the effect of stabilizer concentration on the prepared 5-FU-PLGNPs (F225) at 2% PVA, which exhibited a narrow size distribution compared to the prepared 5-FU-PLGNPs (F525) at 0.5 percent PVA.

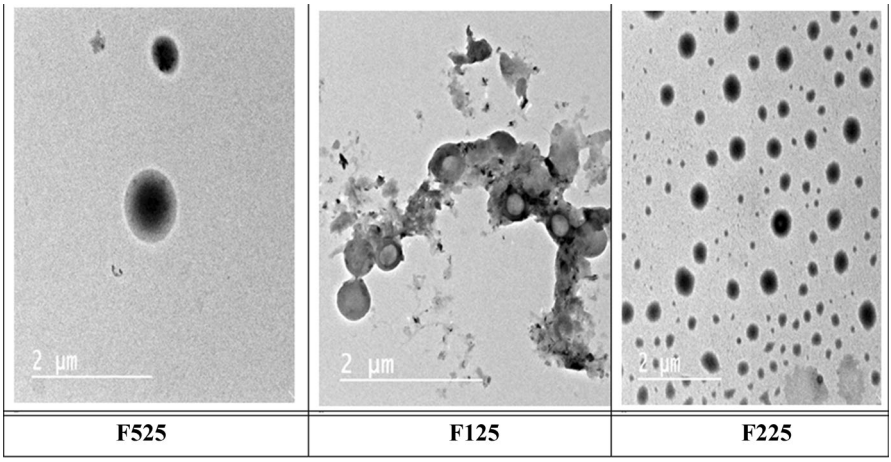


**Fig. 7** TEM photos of 5-FU –PLGNPs (F525, F125 and F225)

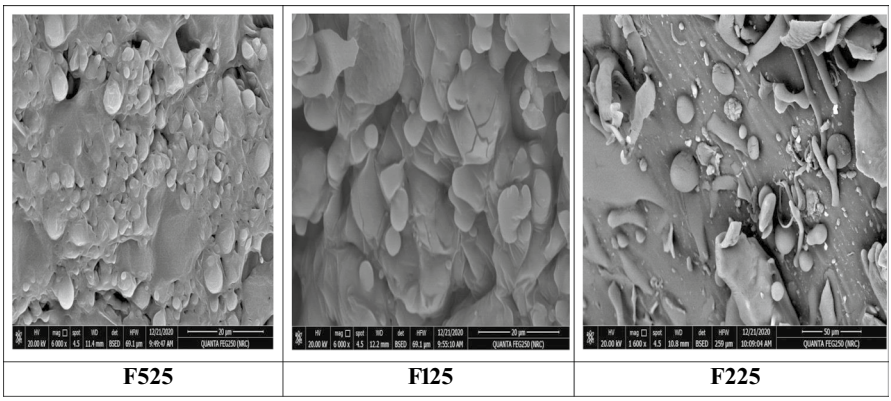


**Fig. 8** SEM images of samples F525, F125, and F225

## EDAX analysis

The existence of an element in a formulation can be determined via EDAX analysis. Figure 9 shows the labeled peaks of EDAX analysis indicating the percentage of elemental of the compounds in the region of interest for the synthesized 5-FU-PLGNPs (F525, F125, and F225). Carbon (49.87, 46.49, and 50.69%), oxygen (47.91, 51.49, and 47.52%), and fluorine atoms (2.32, 2.02, and 1.89%) were found in the region subjected to EDAX analysis of the 5-FU loaded formulation, indicating the formation of 5-FU loaded PLGNPs and the presence of 5-FU within the PLGA matrix.

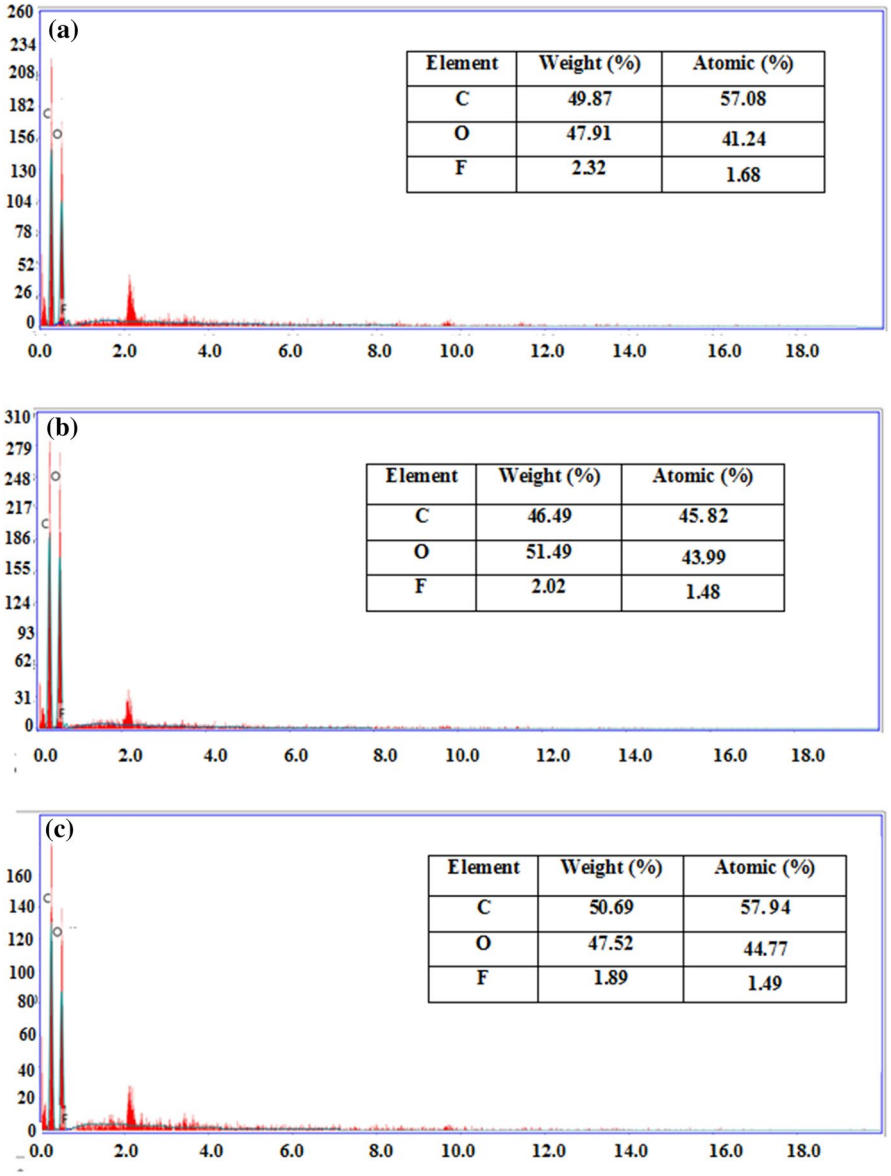


**Fig. 9** EDAX analysis of 5-FU- PLGNPs (F525, F125 and F225)

### In vitro drug release

Dialysis bags were used to perform an in vitro release investigation.. The release of 5-FU was assessed from PLGNPs into PBS (pH 7.4). We made preliminary study of release of 5-FU from 5-FU-PLGNPs using three best formulations at specified parameter at constant 5-FU concentration (25 mg/ml) and different PVA concentration 0.5, 1 and 2% respectively as F525, F125 and F225. The three formulations (i.e. F525, F125 and F225) have high encapsulation efficiency (EE %) as 32.13, 23.56, and 24.8%, respectively and it have particle size as 285, 278.4 and 212 nm, respectively. The in vitro release profiles of 5-FU from PLGNPs (Fig. 10) revealed that pure 5-FU was released more rapidly than the 5-FU-PLGNPs formulations release curve. The release profile demonstrated that 5-FU-PLGANPs formulations reached 10.35–13.76% after 48 h this agree with the same results of Ramchandani, M and Robinson, D. 1998 [53]. For drug loading at 25% mg/ml, in vitro release was biphasic [54]. This is due to a strong chemical interaction between the drug molecule and PLGA, which prevents 5-FU from diffusing into the Phosphate buffer solution. Also, the highest release is encountered by F225 followed by F125 then F525. The percent content released after 48 h reached 13.76% for F225, and 10.53% for F125 the least value; 13.17% for F525. The reason behind the high release from F225 is the small particle size which offers a large surface area for the release of the encapsulated 5-FU therefore facilitating higher 5-FU dissolution. So that formulation F225 showing small particle size and highest content released after 24 h, is the optimized formulation.

### Antiproliferative activity

Using the MTT assay, three nano-preparations were tested in vitro for their activity on HCT-116, HepG-2, and MCF-7 human cancer cells, as well as one human healthy cell line (BJ-1). The percentages of intact cells were counted and compared to those in the control. The activity of the three nano-preparations against the three cancer cell lines was compared to that of doxorubicin. All nano-preparations inhibited the

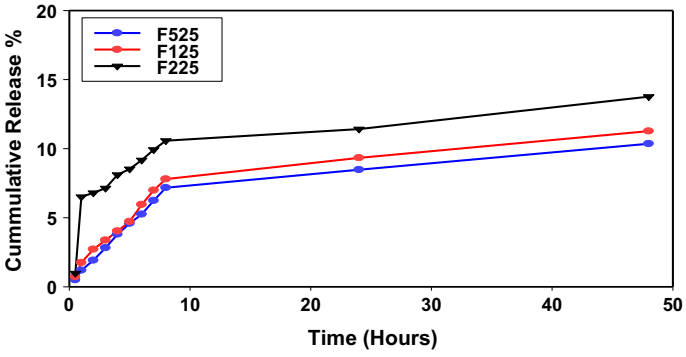


**Fig. 10** Drug release profile of 5-FU from 5-FU- PLGNPs for (F525, F125 and F225)

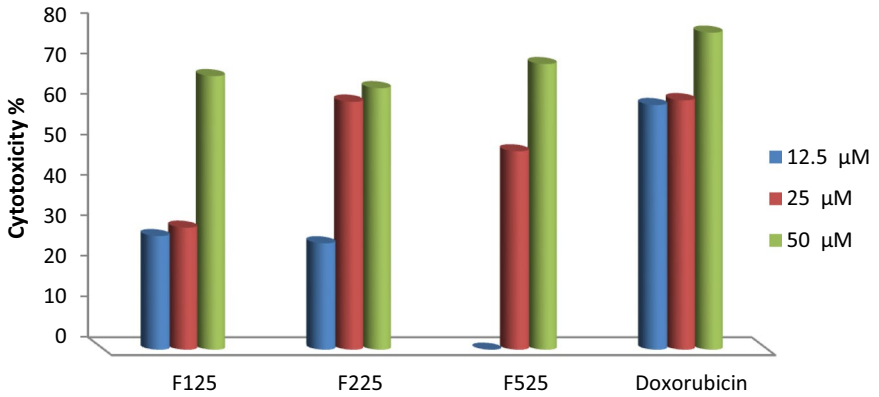


**Fig. 11** Dose -dependent antiproliferative data of the three nano-preparations on HCT-116 cancer cells using the MTT assay after 48 h of exposure

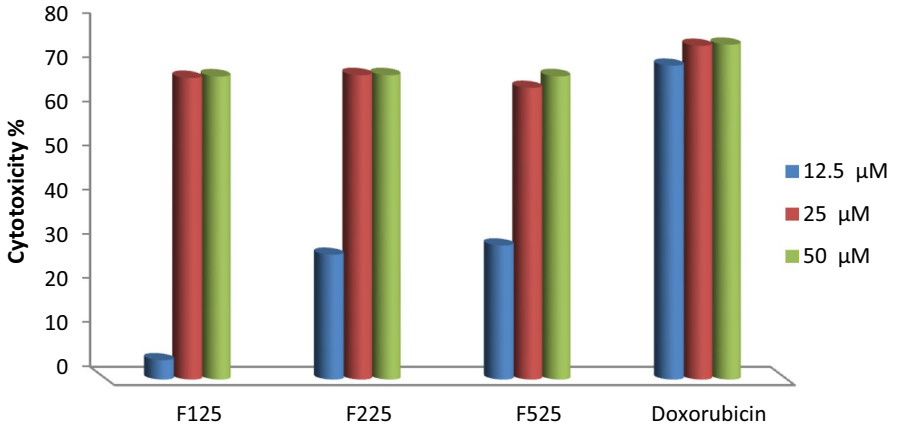


**Fig. 12** Dose-dependent antiproliferative data of the three nano-preparations on MCF-7 cancer cells using the MTT assay after 48 h of exposure

**Table 2** The antiproliferative $IC_{50}$ of the three nano-preparations on the three cancer cell lines using the MTT assay

| Compound code | $IC_{50}$ (µM) ± SD | | |
|---|---|---|---|
| | HCT-116 | HepG-2 | MCF-7 |
| F125 | 37.6 ± 4.1 | 61.7 ± 5.6 | 34.4 ± 3.6 |
| F225 | 28.3 ± 3.1 | 73.4 ± 6.3 | 28.9 ± 2.9 |
| F525 | 40.5 ± 3.7 | 57.8 ± 5.5 | 29.1 ± 3.2 |
| Doxorubicin | 21.8 ± 2.9 | 63.2 ± 5.8 | 16.7 ± 1.5 |

three cancer cells in a dose-dependent manner (Figs. 11 and 12). In case of human colorectal carcinoma cells (HCT-116): both Fig. 11 and Table 2 show that the three nano-preparations (F225, F125 and F525, respectively) have less cytotoxic activities on HCT-116 relative to that of doxorubicin. In case of human breast cancer cells (MCF-7): the three nano-preparations (F225, F525 and F125, respectively) have less cytotoxic activity against MCF-7 relative to the reference drug (Fig. 12 and Table 2). In case of HepG2 human liver cancer cells. Two nano-preparations (F525, and F125, respectively) have strong activity; only one nano-preparations (F225) has slightly less cytotoxic activity against HepG2 relative to that of doxorubicin (Fig. 13 and Table 2). All nano-preparations were tested against non-tumor fibroblast-derived cell line (BJ-1) and demonstrated very low cytotoxicity. From the above mentioned data compared to the positive controlled (doxorubicin), one can conclude that the nano-preparations are less active on the human breast cancer type. The nano-preparation F225 is selectively active on only the human colon cancer type. The two nano-preparation F525 and F125 are selectively active on only the human liver cancer type.

## Conclusions

In this research, 5-FU-loaded PLGNPs were successfully made using the double emulsion (W1/O/W2) approach, and a number of parameters influencing particle size were investigated, including 5-FU and PLGA concentration for the 1st emulsion and PVA concentration for the second emulsion. With increasing concentrations of 5-FU from 10 to 25 mg/ml, an increase in EE percent values was observed. Increases in EE percent values were also found when the concentration of PVA in the 2nd emulsion was increased from 1 to 2% while the concentration of 5-FU in the first emulsion remained constant. Furthermore, as the amount of PVA is increased, the particle size grows proportionally, although a smaller particle size can be produced at a high 5-FU concentration than at a lower concentration. The surface morphology of the obtained nanoparticles has a smooth surface with a spherical shape, as seen

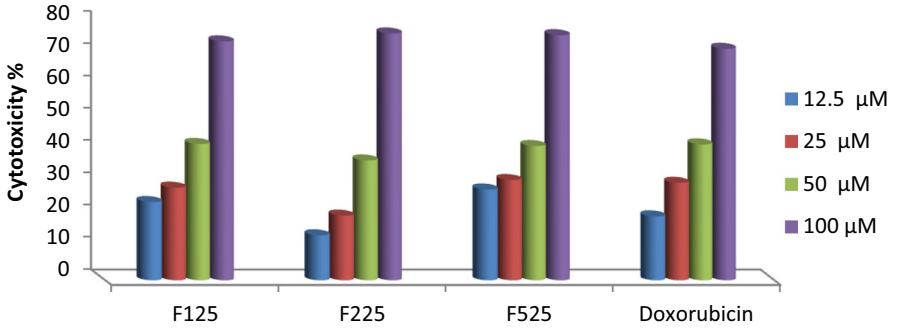


**Fig. 13** Dose-dependent antiproliferative data of the three nano-preparations on HepG2 cancer cells using the MTT assay after 48 h of exposure

by SEM pictures. 5-FU interacts with PLGA, and 5-FU is present in PLGNPs, as demonstrated by FTIR. The molecularly distributed 5-FU in PLGNPs was shown by an XRD investigation. The PLGNPs were shown to be effective in the creation of controlled release matrices for anticancer drugs based on the EE percent of 5-FU in the PLGA matrix. The optimized NPs (F225) had the highest EE % and smallest particle size, which helped to delay drug release and sustain 5-FU release, which was determined to be ideal for a stable monodispersed and confirmed by in vitro release. All nano preparations were tested against non-tumor fibroblast-derived cell line (BJ-1) and demonstrated very low cytotoxicity compared to the positive controlled (doxorubicin).the nano-preparations are less active on the human breast cancer type. The nano-preparations F225 is selectively active on only the human colon cancer type. The two nano-preparations F525 and F125 are selectively active on only the human liver cancer type.

**Author's contributions** MS was involved in conceptualization, methodology, investigation, resources, data curation, writing-original draft and editing writing-reviewing and editing. HMA contributed to methodology. HMA conducted the biological assays and provided the experimental procedures and results of biological part. MMHA was involved in conceptualization, funding acquisition.

**Funding** Open access funding provided by The Science, Technology & Innovation Funding Authority (STDF) in cooperation with The Egyptian Knowledge Bank (EKB).

## Declarations

**Conflict of interest** The authors report no declarations of interest.



## References

1. Nagai H, Kim YH (2017) Cancer prevention from the perspective of global cancer burden patterns. Thorac Dis 9(3):448–451
2. Ozols RF et al (2007) Clinical cancer advances 2006: major research advances in cancer treatment, prevention, and screening-a report from the American Society of Clinical Oncology. J Clin Oncol 25(1):146–162
3. Hubbell JA (2003) Materials science. enhancing drug function. Science 300(5619):595–596
4. Cai C et al (2006) Enhanced liver targeting of 5-fluorouracil using galactosylated human serum albumin as a carrier molecule. J Drug Traget 14(2):55–61
5. Kubota T (1999) Recent progress in combination therapy of low-dose CDDP/5-FU in Japan. theoretical basis for low-dose CDDP/5-FU therapy. Jpn J Cancer Chemother 26:1536–1541

6. Cao S, Rustum YM (2000) Synergistic antitumor activity of irinotecan in combination with 5-fluorouracil in rats bearing advanced colorectal cancer: role of drug sequence and dose. Cancer Res 60:3717–3721
7. Shapiro WR et al (1992) A randomized comparison of intra-arterial versus intravenous with or without intravenous 5-fluorouracil, for newly diagnosed patients with malignant glioma. J Neurosurg 76(5):772–781
8. Tummala S et al (2014) Preparation, physicochemical characterization and in vitro evaluation of oxaliplatin solid lipid nanoparticles for the treatment of colorectal cancer. Indo Am J Pharm Res 4:3579–3587
9. Tummala S et al (2016) 5-Fluorouracil enteric-coated nanoparticles for improved apoptotic activity and therapeutic index in treating colorectal cancer. Drug Delivery 23(8):2902–2910
10. Longley DB, Harkin DP, Johnston PG (2003) 5-fluorouracil: mechanisms of action and clinical strategies. Nat Rev Cancer 3(5):330–338
11. Parker WB, Cheng YC (1990) Metabolism and mechanism of action of 5-fluorouracil. Pharmacol Ther 48(3):81–395
12. Di Paolo A et al (2001) Relationship between 5-fluorouracil disposition, toxicity and dihydropyrimidine dehydrogenase activity in cancer patients. Ann Oncol 12(9):1301–1306
13. van Kuilenburg AB et al (2000) Clinical implications of dihydropyrimidine dehydrogenase (DPD) deficiency in patients with severe 5-fluorouracil-associated toxicity: identification of new mutations in the DPD gene. Clin Cancer Res 6(12):4705–4712
14. Zhang J et al (2016) Antitumor activity of electrospun polylactide nanofibers loaded with 5-fluorouracil and oxaliplatin against colorectal cancer. Drug Deliv 23(3):784–790
15. Arias JL et al (2008) Poly (alkylcyanoacrylate) colloidal particles as vehicles for antitumour drug delivery: a comparative study. Colloids Surf B 62(1):64–70
16. Zhang N et al (2008) 5-Fluorouracil: mechanisms of resistance and reversal strategies. Molecules 13(8):1551–1569
17. Sahle FF et al (2016) Formulation and in vitro evaluation of polymeric enteric nanoparticles as dermal carriers with pH-dependent targeting potential. Eur J Pharm Sci 92:98–109
18. Mora-Huertas CE, Fessi H, Elaissari AJ (2010) Polymer-based nanocapsules for drug delivery. Int J Pharm 385(1–2):113–142
19. Lamprecht A et al (2001) Biodegradable nanoparticles for targeted drug delivery in treatment of inflammatory bowel disease. J Pharmacol Expt Ther 299(2):775–781
20. Lee JS et al (2004) Degradation behaviour in vitro for poly (D, L-lactide-co-glycolide) as drug carrier. Biomed Mater Eng 14(2):185–192
21. Li X et al (2008) PLGA nanoparticles for the oral delivery of 5-Fluorouracil using high pressure homogenization-emulsification as the preparation method and in vitro/in vivo studies. Drug Dev Ind Pharm 34(1):107–115
22. Kim JH et al (2008) Antitumor efficacy of cisplatin-loaded glycol chitosan nanoparticles in tumor-bearing mice. J Control Release 127(1):41–49
23. Upadhyay KK et al (2010) The intracellular drug delivery and anti tumor activity of doxorubicin loaded poly (γ-benzyl l-glutamate)-b-hyaluronan polymersomes. Biomaterials 31(10):2882–2892
24. Zhu Z et al (2010) Paclitaxel-loaded poly (N-vinylpyrrolidone)-b-poly (ε-caprolactone) nanoparticles: preparation and antitumor activity in vivo. J Control Release 142(3):438–446
25. Li S et al (2008) Pharmacokinetic characteristics and anticancer effects of 5-fluorouracil loaded nanoparticles. BMC Cancer 8(1):1–9
26. Selvaraj V, Alagar MJ (2007) Analytical detection and biological assay of antileukemic drug 5-fluorouracil using gold nanoparticles as probe. Int J Pharm 337(1–2):275–281
27. Narayanan K, Subrahmanyam V, Venkata Rao JJ (2014) A fractional factorial design to study the effect of process variables on the preparation of hyaluronidase loaded PLGA nanoparticles. Enzyme Research 2014:1–10. https://doi.org/10.1155/2014/162962
28. Guo Y, Shalaev E, Smith SJ (2013) Physical stability of pharmaceutical formulations: solid-state characterization of amorphous dispersions. Trends Anal Chem 49:137–144
29. Samy M et al (2020) Eco-friendly route for encapsulation of 5-fluorouracil into polycaprolactone nanoparticles. Egypt J Chem 63(1):255–267
30. Mo L et al (2012) Preparation and characterization of teniposide PLGA nanoparticles and their uptake in human glioblastoma U87MG cells. Int J Pharm 436(1–2):815–824
31 Mu L, Feng S-S (2003) PLGA/TPGS nanoparticles for controlled release of paclitaxel: effects of the emulsifier and drug loading ratio. Pharm Res 20(11):1864–1872

32 Samy M et al (2021) In vitro release and cytotoxicity activity of 5-fluorouracil entrapped polycaprolactone nanoparticles. Polymer Bulltein. https://doi.org/10.1007/s00289-021-03804-9
33. Rauta PR et al (2016) Enhanced efficacy of clindamycin hydrochloride encapsulated in PLA/PLGA based nanoparticle system for oral delivery. IET Nano Biotechnol 10(4):254–261
34. Samy M et al (2020) Formulation, characterization and in vitro release study of 5-fluorouracil loaded chitosan nanoparticles. Int J Bio Macromol 156:783–791
35. Abd-El-Maksoud M et al (2020) Chemistry of phosphorus ylides Part 47 synthesis of Organophosphorus and Selenium Pyrazolone derivatives, their antioxidant activity, and Cytotoxicity against MCF7 and HepG2. Russian J General Chem 90(12):2356–2364
36. Abuelizz HA et al (2020) Antiproliferative and antiangiogenic properties of new VEGFR-2-targeting 2-thioxobenzo [g] quinazoline derivatives (in vitro). Molecules 25(24):5944
37. Elatif RA et al (2020) Chemical composition and biological activity of Salicornia fruticosa L. Egypt J Chem 63(5):1713–1721
38. AminA, et al (2018) Assessment of formulation parameters needed for successful vitamin C entrapped polycaprolactone nanoparticles. Int J Polym Mater Polym Biomater 67(16):942–950
39. Thomasin C et al (1996) Tetanus toxoid and synthetic malaria antigen containing poly (lactide)/poly (lactide-co-glycolide) microspheres: importance of polymer degradation and antigen release for immune response. J Control Release 41(1–2):131–145
40. Rösler A, Vandermeulen G, Klok HA (2001) Advanced drug delivery devices via self-assembly of Amphiphilic Block Copolymers. Adv Drug Deliv Rev 53:95–108
41. Santhi K et al (2005) Development and In-vitro evaluation of a topical drug delivery system containing Betamethazone loaded ethyl cellulose nanospheres. Trop J Pharm Res 4(2):495–500
42. Dubey RD et al (2016) PLGA nanoparticles augmented the anticancer potential of pentacyclic triterpenediol in vivo in mice. RSC Adv 6(78):74586–74597
43. Gracia E et al (2018) Improvement of PLGA loading and release of curcumin by supercritical technology. J Supercritical Fluids 141:60–67
44. Shaker MN et al (2014) Enhanced photodynamic efficacy of PLGA-encapsulated 5-ALA nanoparticles in mice bearing Ehrlich ascites carcinoma. Appl Nanosci 4(7):777–789
45. Singh G et al (2018) Spectral analysis of drug loaded nanoparticles for drug-polymer interactions. J Drug Deliv Therap 8(6):111–118
46. Colthup NB, Daly LH, Wiberley SE (1975) Introduction to infrared and Raman spectroscopy. Academic Press, New York
47. Khodaverdi S et al (2020) Evaluating inhibitory effects of paclitaxel and vitamin D3 loaded poly lactic glycolic acid co-delivery nanoparticles on the breast cancer cell line. Adv Pharm Bull 10(1):30
48 Tığlı Aydın RS, Pulat M (2012) 5-Fluorouracil encapsulated chitosan nanoparticles for pH-stimulated drug delivery: evaluation of controlled release kinetics. J Nanomater 2012:1–10
49. Ashour AE et al (2019) Physical pegylation enhances the cytotoxicity of 5-fluorouracil-loaded PLGA and PCL nanoparticles. Int J Nanomedicine 14:9259–9273
50. Olukman M, Solak EK (2012) Release of anticancer drug 5-Fluorouracil from different ionically crosslinked alginate beads. J Biomater Nanobiotechnol 3(04):469
51. Nair L et al (2011) Biological evaluation of 5-fluorouracil nanoparticles for cancer chemotherapy and its dependence on the carrier. PLGA. Int J Nanomed 6:1685
52. Silva MF et al (2015) Study of thermal degradation of PLGA, PLGA nanospheres and PLGA/maghemite superparamagnetic nanospheres. Mater Res 18:1400–1406
53. Ramchandani M, Robinson DJ (1998) In vitro and in vivo release of ciprofloxacin from PLGA 50: 50 implants. J Control Release 54(2):167–175
54 Sanders LM et al (1985) Controlled delivery of an LHRH analogue from biodegradable injectable microspheres. J Control Release 2:187–195